Published in final edited form as:
Int J Cardiol. 2013 November 30; 169(6): 394–401. doi:10.1016/j.ijcard.2013.10.021.

Synergistic Effect of Local Endothelial Shear Stress and Systemic Hypercholesterolemia on Coronary Atherosclerotic Plaque Progression and Composition in Pigs

Konstantinos C. Koskinas, MD[a,b,*], **Yiannis S. Chatzizisis, MD, PhD**[a,b,*], **Michail I. Papafaklis, MD, PhD**[a,b], **Ahmet U. Coskun, PhD**[c], **Aaron B. Baker, PhD**[b], **Petr Jarolim, MD, PhD**[a], **Antonios Antoniadis, MD, PhD**[a], **Elazer R. Edelman, MD, PhD**[a,b], **Peter H. Stone, MD**[a], and **Charles L. Feldman, ScD**[a]

[a]Cardiovascular Division, Brigham and Women's Hospital, Harvard Medical School, Boston, MA

[b]Harvard-MIT Division of Health Sciences & Technology, Massachusetts Institute of Technology, Cambridge, MA

[c]Mechanical and Industrial Engineering, Northeastern University, Boston, MA

Abstract

Background—Systemic risk factors and local hemodynamic factors both contribute to coronary atherosclerosis, but their possibly synergistic inter-relationship remains unknown. The purpose of this natural history study was to investigate the combined in-vivo effect of varying levels of systemic hypercholesterolemia and local endothelial shear stress (ESS) on subsequent plaque progression and histological composition.

Methods—Diabetic, hyperlipidemic swine with higher systemic total cholesterol (TC) (n=4) and relatively lower TC levels (n=5) underwent three-vessel intravascular ultrasound (IVUS) at 3–5 consecutive time-points in-vivo. ESS was calculated serially using computational fluid dynamics. 3-D reconstructed coronary arteries were divided into 3mm-long segments (n=595), which were stratified according to higher vs. relatively lower TC and low (<1.2 Pa) vs. higher local ESS (≥1.2 Pa). Arteries were harvested at 9 months, and a subset of segments (n=114) underwent histopathologic analyses.

Address for Correspondence: Peter H. Stone, M.D., Cardiovascular Division, Brigham and Women's Hospital, Harvard Medical School, 75 Francis Street, Boston, MA 02115, Tel: 857 307 1963, Fax: 857 307 1955, pstone@partners.org.
*The first two authors contributed equally to this work

All authors take responsibility for all aspects of the reliability and freedom from bias of the data presented and their discussed interpretation

Conflicts of Interest: None

The authors of this manuscript have certified that they comply with the Principles of Ethical Publishing in the International Journal of Cardiology [41].

Results—Change of plaque volume (ΔPV) by IVUS over time was most pronounced in low-ESS segments from higher-TC animals. Notably, higher-ESS segments from higher-TC animals had greater ΔPV compared to low-ESS segments from lower-TC animals ($p<0.001$). The time-averaged ESS in segments that resulted in significant plaque increased with increasing TC levels (slope: 0.24 Pa/100mg/dl; $r=0.80$; $p<0.01$). At follow-up, low-ESS segments from higher-TC animals had the highest mRNA levels of lipoprotein receptors and inflammatory mediators and, consequently, the greatest lipid accumulation and inflammation.

Conclusions—This study redefines the principle concept that "low" ESS promotes coronary plaque growth and vulnerability by demonstrating that: (i.) the pro-atherogenic threshold of low ESS is not uniform, but cholesterol-dependent; and (ii.) the atherogenic effects of local low ESS are amplified, and the athero-protective effects of higher ESS may be outweighed, by increasing cholesterol levels. Intense hypercholesterolemia and very low ESS are synergistic in favouring rapid atheroma progression and high-risk composition.

Keywords

coronary atherosclerosis; endothelial shear stress; hypercholesterolemia; intravascular ultrasound; histology

1. Introduction

Atherosclerosis results from a complex interplay between systemic risk factors and locally acting stimuli. Systemic hypercholesterolemia largely determines an individual's propensity to coronary artery disease (CAD) [1,2], whereas local hemodynamic factors, low endothelial shear stress (ESS) in particular, dictate the highly focal and heterogeneous atherosclerotic manifestations in susceptible individuals [3–11]. While the relative contribution of systemic and local pro-atherogenic factors to coronary atherosclerosis has been long established, this study explored an important issue not addressed in previous investigations: the *combined* effect of different levels of both hypercholesterolemia and local ESS on the natural history of CAD.

Low ESS [3,5,6], and high cholesterol levels [12] both promote endothelial dysfunction *in vitro*, thus raising the translational hypothesis of a complementary or even synergistic pro-atherogenic effect of hypercholesterolemia and local ESS *in vivo*. Compelling evidence has indeed suggested that cholesterol levels modify the effect of blood flow on atherogenesis [13–15]. Previous studies, however, used cultured cells, which lack the complex environment of the atherosclerotic vascular wall *in vivo*, or examined, in a cross-sectional fashion, non-coronary arteries of atherosclerotic mice which have major differences from human coronary plaques [16]. Currently, it is unknown how the intensity of hypercholesterolemia modifies the pathobiologic effect of low ESS in a human-like model of experimental CAD.

The clinical value of identifying early, within at-risk individuals, which coronary arterial regions are most prone to subsequent development of vulnerable plaque cannot be overemphasized. Preclinical and clinical studies have consistently demonstrated that low ESS predicts plaque enlargement [4,10,17] and destabilization [11,18,19], but they have also

raised several important issues. First, the profound variability of atherosclerotic manifestations in arterial regions with similar atherosclerosis-prone hemodynamic characteristics suggests that the impact of low local ESS may be affected by other factors concomitantly influencing atherosclerosis. Second, while local ESS is a measurable predictor of subsequent plaque behavior [4], no uniform values have been identified to discriminate “low” (athero-prone) vs. “physiologic” (athero-protective) ESS magnitude. To address these key unresolved issues, the present analysis explored whether the magnitude of hypercholesterolemia affects the threshold below which local ESS influences the progression and morphology of coronary plaque in vivo.

The purposes of this serial study were: (i.) to prospectively characterize *in vivo* the combined effect of varying levels of systemic blood cholesterol and local ESS on the evolution and histological composition of heterogeneous coronary lesions; (ii.) to explore potential mechanisms underlying the combined atherogenic effects of hypercholesterolemia and local ESS; and (iii.) to test the hypothesis that the combination of local ESS and systemic cholesterol levels has incremental value for prediction of rapid plaque progression and high-risk plaque development. For our analyses we employed two complementary approaches: we serially profiled regional ESS and plaque progression *in vivo*, and then performed histopathological analyses, in the coronary arteries of animals with varying degrees of hypercholesterolemia. We utilized an established hypercholesterolemic, diabetic pig model capable of developing coronary lesions very similar to those observed in humans [20,21]. Although the serum cholesterol values in these animals were markedly elevated per protocol, the individual variation of the animals’ cholesterol levels allowed for detailed investigation of the effect of different systemic cholesterol and local ESS values on coronary atherosclerosis.

2. Methods

2.1. Pig model of coronary atherosclerosis

The experimental protocol conforms to the Guide for the Care and Use of Laboratory Animals (US National Institutes of Health Publication 85–23, revised 1996) and was approved by the Harvard Medical School Institutional Animal Care and Use Committee. All animals received humane care. We utilized two animal cohorts used in studies investigating the natural history of CAD in pigs [17–19]. Briefly, nine male Yorkshire pigs were rendered diabetic by injection of streptozotocin and fed a high-fat diet [20]. The first cohort included five pigs followed for 36 weeks [17], and the second cohort included four pigs followed for 30 weeks [18,19]. No animals in this study received medications that could influence atherosclerosis [18]. For the present analysis, animals were categorized into a higher total cholesterol (TC) group (n=4) and a relatively lower-TC group (n=5), using the median of all animals’ TC values (762mg/dl) as the cut point.

2.2. Study protocol

The study protocol is summarized in Supplemental Figure 1. Three-vessel coronary angiography and intravascular ultrasound (IVUS) were serially performed *in vivo* at five consecutive time points in the 36-week cohort (T_1= 4 weeks; T_2=11 weeks; T_3=16 weeks;

T_4=23 weeks; and T_5=36 weeks) [17], and at three time points in the 30-week cohort (T_3=16 weeks; T_4=23 weeks; and T_5=30 weeks) [18,19]. Animals were sacrificed immediately following the final catheterization (T_5) with iv injection of EUTHASOL (Virbac AH, 150 mg/kg) while anesthetized, and their coronary arteries – which had previously been serially profiled in vivo – were harvested, frozen in liquid nitrogen, and stored at −80°C until further analysis by histopathology, immunohistochemistry, and RT-PCR.

2.3. In vivo vascular profiling for ESS calculation

Vascular profiling methodology combining IVUS and biplane coronary angiography for 3D reconstruction of the arterial anatomy and for ESS calculation has been described and validated *in vivo* in animals [17–19] and humans [4,9,22]. The arterial lumen and external elastic membrane (EEM) were segmented from digitized, end-diastolic IVUS images. The physical 3D path of the IVUS transducer during pullback was reconstructed using the corresponding biplane angiographic projections, and the segmented IVUS images were located along this path and oriented appropriately. Lumen and EEM boundary points were connected by spline curves to accurately rebuild the lumen and EEM geometry in 3D space, respectively. Coronary blood flow was calculated directly from the time required for the previously calculated, true 3D volume of blood contained within the arterial section to be displaced by radio-opaque material during a contrast injection. The detailed intravascular flow characteristics were obtained by solving the transport equations governing the conservation of mass and momentum (Phoenics, CHAM, England). ESS at the lumen surface of the reconstructed arteries was calculated at all time-points with computational fluid dynamics as the product of blood viscosity (calculated from the measured hematocrit) and the gradient of blood velocity at the wall. The processes of data acquisition and analysis are highly reproducible [23].

Reconstructed arteries were divided sequentially, in a completely nonbiased manner, into consecutive 3-mm-long segments along their length starting at the ostium. We used 3mm-long segments as our unit of measure because this length would accurately reflect the local hemodynamic characteristics and the highly focal changes occurring within the plaque over time, and because ESS [17,18] and histological characteristics [24] are essentially homogeneous within such short segments. Matching the same segments over multiple consecutive time-points was based on the anatomical location of readily visible IVUS-derived landmarks (side branches) [4,17,22]. The same landmarks were subsequently identified on the preserved arteries, allowing for identification of the corresponding physical location of each segment [18,19].

Mean ESS was calculated in each 3-mm-long segment at each individual time-point. Because local ESS in individual segments often changed over time in response to plaque and remodeling progression [17], we also assessed the time-averaged local ESS throughout the study period, to account for each segment's lifetime exposure to variable ESS over time. ESS at each time-point, as well as the time-averaged ESS over time, were categorized as low (<1.2Pa) or higher ESS (≥1.2Pa) for each segment, applying a cut point previously used in animals [17] and humans [22]. In addition to the dichotomization of ESS as low ESS (<1.2Pa) vs. higher ESS (≥1.2Pa), we also performed an ancillary analysis using the

quartiles of time-averaged ESS, to assess possible dose-response associations between local ESS and subsequent plaque growth.

2.4. Serial assessment of plaque progression in vivo by IVUS

The 3D geometry of the plaque (plaque plus media) in the reconstructed arteries was taken as the difference between the outer vessel wall and the lumen. Plaque progression by IVUS was measured serially in each 3mm segment between consecutive time-points ($T_2 \rightarrow T_3$; $T_3 \rightarrow T_4$; $T_4 \rightarrow T_5$) by the change of plaque volume (ΔPV). To account for the different duration among consecutive temporal intervals we calculated time-normalized, weekly changes of plaque volume (nΔPV = ΔPV/week) for all time intervals according to the following equation:

$$\text{Normalized } \Delta\text{PV} = \frac{\Delta\text{PV}}{\text{Duration of time interval (weeks)}}$$

Using the same equation, we also calculated the time-normalized plaque progression in each segment throughout the study period ($T_2 \rightarrow T_5$). At follow-up (T_5), segments with maximum intima-media thickness (maxIMT) ≥0.5mm were considered as segments with significant plaque by IVUS [17,25].

2.5. Histopathologic analyses

While plaque progression by IVUS was measured serially and was time-normalized, histology could be performed only upon animal sacrifice, i.e., at a time-point (T_5) that differed in the 36-week vs. 30-week cohort. We therefore performed a histologic sub-study in the 36-week cohort only, so that analyzed animals were exposed to atherogenic experimental conditions over the same 36-week timeframe, thus allowing for meaningful histopathologic comparisons at follow-up. Histopathology, immunostaining, and gene expression experiments were performed for the purposes of this study in 114 segments with previously identified *in vivo* ESS. These segments were carefully selected to represent different ESS over time and had a broad range of 3D geometry and plaque by IVUS.

We determined the lipid accumulation and inflammatory cell infiltration in relation to the local ESS and systemic TC, because lipid content and inflammation are features of high-risk plaques that rupture and trigger acute coronary thrombosis in humans [2,26]. The middle portion of each segment was cryosectioned at 7μm thickness. Lipid content and leukocyte infiltration were assessed by Oil-Red-O staining and CD45-immunostaining (mouse anti-pig CD45, clone K252-1E4, AbD Serotec, Oxford, UK; 1:50), respectively. Quantitative analyses were performed on Image-Pro Plus 5.1 (Media Cybernetics, Bethesda, MD).

2.6. Measurement of gene expression by RT-PCR

Cryosections from each segment were harvested, and the mRNA from the intima and media was isolated (Qiagen, Valencia, CA) and reverse transcribed (Invitrogen, Carlsbad, CA). Real-time RT-PCR was performed and target gene mRNA levels were normalized to the “housekeeping” (GAPDH) mRNA level in each extract. We measured mRNA levels of the LDL-receptor (LDL-R), lectin-like oxidized LDL receptor-1 (LOX-1), lipoprotein-

associated phospholipase-A_2 ($LpPLA_2$), vascular cellular adhesion molecule-1 (VCAM-1), and monocyte chemotactic protein-1 (MCP-1). The primers used are shown in Supplemental Table 1.

2.7. Biochemical analyses

The lipid profile [TC, low-density lipoprotein cholesterol (LDL-C), high-density lipoprotein cholesterol (HDL-C)] and blood glucose were assessed every month following overnight (≥12 hours) fasting. To assess the lifetime exposure to hypercholesterolemia and hyperglycemia, the time-average of all serial TC, LDL-C, HDL-C, and glucose measurements was calculated. Lipid profiles were measured using assays developed for human use (Roche Diagnostics, Indianapolis, IN).

2.8. Study assessments

We assessed serial plaque progression by IVUS over time and histopathological plaque characteristics at follow-up in segments stratified according to low ESS (<1.2 Pa) vs. higher ESS (≥1.2 Pa) and higher- vs. relatively lower systemic TC. We employed a composite approach to associate local ESS with subsequent plaque characteristics: (**i**) ESS at each time-point was related to subsequent plaque progression by IVUS between consecutive time-points; (**ii**) the time-averaged ESS over time was related to the mean rate of plaque progression by IVUS throughout the study period; and (**iii**) the time-averaged ESS over time was related to histopathologic plaque characteristics at sacrifice.

2.9. Statistical analyses

Statistical analyses were performed using SPSS version 18.0 (SPSS Inc., Chicago, IL). Continuous variables are summarized as mean ± standard error of the mean (SEM), and categorical variables as actual numbers and percentages. For analyses with a continuous dependent and a categorical independent variable, random effects analysis of variance was used. Since observations were not statistically independent, animals and individual arteries were declared as random effects to account for the clustering of segments within arteries and animals. Linear regression was used for both continuous independent and dependent variables. The Huber-White sandwich estimator was used to correct for the clustering of arteries within animals. Findings were considered statistically significant at the 0.05 level.

3. Results

The time-averaged TC was 852±32 mg/dL for the higher-TC group vs. 658±34 mg/dL for the relatively lower-TC group (p=0.016). Higher-TC animals had higher LDL-C (669±53 vs. 501±47 mg/dL; p=0.02), but similar HDL-C levels (213±23 vs. 163±16 mg/dL, respectively; p=0.56). Blood glucose levels did not differ between the two groups (252±28 vs. 220±31 mg/dL; p=0.64).

Twenty seven coronary arteries from nine pigs were serially profiled (left anterior descending, n=9; left circumflex, n=9; right coronary artery, n=9). Arteries were divided into a total of 595 3mm-long segments: 237 segments from the 12 arteries of the higher-TC animals and 358 segments from the 15 arteries of the relatively lower-TC animals.

3.1. Incremental effect of local low ESS and cholesterol levels on coronary plaque progression

For serial measurements of nΔPV by IVUS between consecutive time-points, all segments (n=595) were stratified at each time-point into 4 categories on the basis of low ESS (<1.2 Pa) vs. higher ESS (≥ 1.2 Pa) at the given time-point, and on higher-TC vs. relatively lower-TC of the corresponding animal. Because local ESS in individual segments often changed as plaque formed and progressed [17], the numbers of segments with low ESS vs. higher ESS changed over time. The nΔPV was greater in segments with low ESS vs. higher preceding ESS in each TC group, and it was greater in segments from higher-TC animals with low ESS (<1.2Pa) compared to segments from relatively lower-TC animals with similarly low ESS (Fig. 1A). Intriguingly, nΔPV was more marked in higher-ESS segments from higher-TC animals compared to lower-ESS segments from lower-TC animals for two of the three intervals ($T_2 \rightarrow T_3$ and $T_3 \rightarrow T_4$; Fig. 1A). Fig. 1B shows representative examples of plaque progression by IVUS between consecutive time-points in segments stratified by ESS and TC categories.

Very similar results were obtained when the rate of plaque progression over the entire study period was assessed in relation to the time-averaged ESS. The time-normalized nΔPV was greater in segments with low time-averaged ESS (<1.2 Pa) from higher-TC animals compared to lower-TC animals (Fig. 2A). Of note, the nΔPV was greater in segments with high time-averaged ESS from higher TC animals compared segments with low time-averaged ESS from lower TC animals ($p<0.001$; Fig. 2A). nΔPV was greater in the lower vs. higher quartiles of time-averaged ESS, for both higher-TC animals ($p<0.001$) and relatively lower-TC animals ($p=0.004$; Fig. 2B). Within each ESS quartile, plaque growth was greater in segment from higher-TC compared to lower-TC animals ($p<0.001$ for all quartiles; Fig. 2B).

Together these results indicate that in arterial regions exposed to different cholesterol and local ESS levels: (i.) the low-ESS effect on plaque growth is strongly amplified by increasing cholesterol levels; and (ii.) the athero-protective effect of higher ESS may be outweighed by the stronger pro-atherogenic effect of very intense hypercholesterolemia.

3.2. The pro-atherogenic threshold of local ESS is modified by the magnitude of hypercholesterolemia

We focused on segments that developed significant plaque by IVUS at follow-up (T_5), defined as maxIMT≥0.5mm (n=268 of 595 segments; 45%). The time-averaged ESS in these segments was positively related to the TC of the corresponding animal ($r=0.80$, $p=0.005$; Fig. 3A). The association was even stronger between the time-averaged ESS and the LDL-C levels in each animal ($r=0.84$, $p=0.004$; Fig. 3B). The ESS preceding the formation of significant plaque by IVUS increased by 0.24 Pa for an increase of TC by 100 mg/dl and by 0.23 Pa for an increase of LDL-C by 100 mg/dl (Fig. 3).

3.3. Combined effect of hypercholesterolemia and local ESS on plaque composition

For histopathologic and RT-PCR measurements, analyzed segments (n=114) were stratified into four categories according to low (<1.2Pa) vs. higher (≥1.2Pa) time-averaged ESS over

time, and higher-TC vs. relatively lower TC of the corresponding animal. The mRNA levels of LDL-R and LOX-1 were highest in the low-ESS, higher-TC segments (n=22; 19%) compared to all other segments (Fig. 4A, 4B). VCAM-1 and MCP-1 expression increased in segments with low ESS vs. higher ESS, in both higher-TC and relatively lower-TC animals (Fig. 4C, 4D). The mRNA levels of $LpPLA_2$ – an enzyme implicated in the catabolism of oxidized LDL – did not differ significantly in relation to TC or local ESS.

In both higher-TC and relatively lower-TC animals, low-ESS vs. higher-ESS segments had increased lipid accumulation. Among all segments, lipid accumulation was highest in low-ESS segments from higher-TC animals (Fig. 5A, 5B). Similarly, these low-ESS segments from higher-TC animals showed highest CD45-positive intimal area compared to all other segments (Fig. 5C, 5D).

4. Discussion

This natural history study utilized an established large-animal, human-like model of CAD to assess, for the first time *in vivo*, the combined effect of varying degrees of hypercholesterolemia and local ESS on subsequent coronary plaque progression and morphology. Our major findings are: (**i.**) focal plaque growth and histomorphologic characteristics differ substantially in arterial regions with similarly low ESS but with varying cholesterol levels; (**ii.**) the threshold of “low” (pro-atherogenic) vs. “higher” (athero-protective)” local ESS is not uniform, but cholesterol-dependent: the lower the blood cholesterol, the lower the local ESS that precedes the formation of significant plaque; and (**iii.**) the combination of highest cholesterol and lowest local ESS favors the development of plaques with greatest lipid accumulation and inflammation, which are critical features of high-risk coronary plaque [2,26,27]. Novel evidence presented here concerning the focal expression of lipoprotein receptors and potent inflammatory mediators substantiates our IVUS-based and histological observations. Our results thus advance earlier *in vitro* studies which demonstrated a synergistic pro-atherogenic effect of blood flow and cholesterol levels [13–15] and they provide clinically relevant insight into the *in vivo* interrelationship between the main subject-specific systemic risk factor (i.e., hypercholesterolemia) and the major locally acting pro-atherogenic stimulus (i.e., local ESS) in regulating the localization, growth rate, and composition of coronary atheroma.

While low ESS favors endothelial cell dysfunction [3,5,28], hypercholesterolemia *per se* aggravates shear stress–dependent endothelial functions that promote atherogenesis [12,29–32], thereby suggesting an interrelating pathobiologic role of systemic and local factors in atherosclerosis. Previous studies indeed demonstrated that higher cholesterol levels amplify lipid uptake and plaque inflammation *in vitro* and in regions of mouse aortas exposed to plaque-prone flow patterns [13,14]. The present analysis extends those previous findings by demonstrating prospectively that low ESS and hypercholesterolemia are synergistic in promoting coronary plaque growth and favouring the focal formation of lesions bearing histological features of vulnerability. Our current findings are strengthened by using an experimental model of CAD that recapitulates the human disease much better than atherosclerotic mice; by providing quantitative analyses based on direct ESS computation and volumetric plaque progression in vivo; by profiling serially the highly variable systemic

cholesterol and local ESS environments throughout the evolution of individual coronary lesions; and by demonstrating how these 2 risk factors *in combination* critically influence the evolution of plaques that progress at substantially different rates and result in distinctly different morphologies.

This study expands an understanding of the concept that “low” ESS promotes atherosclerosis, and demonstrates that plaque progression in certain arterial regions with low local ESS may actually be less profound compared to other regions that have higher ESS but are exposed to relatively higher systemic cholesterol. This links to our intriguing finding that the threshold of “low” (athero-prone) vs. “higher” (athero-protective) ESS *in vivo* is not uniform, but it increases with increasing cholesterol levels. Our present results thus indicate that the magnitude of hypercholesterolemia – likely along with other systemic factors – modulates the arterial susceptibility to local ESS and thereby influences the rate of plaque growth in regions which are atherosclerosis-susceptible as a result of their local hemodynamic milieu. The combination of low local ESS and higher cholesterol identifies a small subset of arterial regions that are particularly prone to rapid plaque progression and subsequent plaque vulnerability. Our findings provide some insights into key issues not addressed in prior studies, i.e., (i.) the largely unexplained observation that not all arterial regions exposed to similarly low ESS develop advanced lesions in experimental models [11,17–19]; and (ii.) the clinical conundrum that coronary sites with presumed plaque-prone anatomy (e.g., arterial curvatures or bifurcations) develop highly variable atherosclerosis in individuals with different lipid profiles [1,2,24].

The clinical sequelae of coronary plaques correlate tightly to their composition [2,26,27]. By profiling local ESS serially in developing plaques *in vivo*, and then analyzing the same lesions by histopathology – the gold standard for tissue characterization – we addressed directly the combined effect of hypercholesterolemia and of the long-term ESS milieu on subsequent plaque morphology. An important finding of this study is that the minority of arterial regions exposed to lowest ESS and highest cholesterol gave rise to lesions with greatest lipid accumulation and inflammation – two features of fatally disrupted human coronary plaques [27]. Low ESS in combination with higher cholesterol levels associated with increased expression of lipoprotein receptors (LDL, LOX-1). In addition, low-ESS regions co-localized with increased expression of VCAM and MCP-1, which are potent regulators of leukocyte adhesion and migration, respectively. These findings agree with prior studies *in vitro* and in small animal models of atherosclerosis [11,33–35]. Thus, in low-ESS arterial regions where the endothelium was more receptive to circulating cholesterol, intimal lipid accumulation was determined by the magnitude of hypercholesterolemia. While we found no cholesterol effect on VCAM-1 or MCP-1 expression, our finding of greater inflammation in low-ESS segments exposed to higher- vs. relatively lower cholesterol might relate to an enhanced inflammatory response to greater lipid accumulation [36], and to the induction of LOX-1 – a multifunctional receptor known to promote plaque inflammation [37,38].

Our present analysis may have potential clinical implications. Recent experimental [17,18] and clinical investigations [4,10,22] consistently demonstrated that *in vivo* calculated low ESS predicts subsequent plaque enlargement early in its natural history – findings which

might eventually allow for preemptive strategies to alter the natural history of high-risk plaque and avert adverse cardiac events [39,40]. Our current results now advance those previous insights by highlighting the incremental value of the combination of local ESS and systemic cholesterol levels vs. local ESS alone for prediction of plaque growth and vulnerability. Determination of a numerical threshold of "low" ESS to identify *in vivo*, in a given individual, which arterial regions are most prone to atherosclerosis may require adjustment for the subject-specific levels of blood cholesterol.

The present investigation is limited by being a post hoc exploratory analysis; nevertheless, it provides a proof of concept of the interrelationship between systemic and local pro-atherogenic stimuli in the natural history of CAD. The use of a larger number of pigs would have been beneficial, if feasible, but the statistical power increased by profiling the entire length of 27 arteries, divided into 595 segments serially at multiple time-points. While the pig model is an excellent model to study human coronary atherosclerosis [20,21], the present results may not be entirely generalizable to human CAD where the cholesterol values are much lower. While cholesterol levels were substantially elevated even in the relatively lower-TC animals, we still found statistically significant differences associated with the relative magnitude of hypercholesterolemia. Segments that were analyzed by histopathology were not randomly selected; the selection bias was substantially limited, however, by intentionally selecting segments with different ESS magnitude and different plaque progression by IVUS over time, so that the entire spectrum of ESS values and atherosclerotic plaques was represented. Diabetes likely accelerated plaque growth and modulated plaque composition; glucose levels, however, did not differ between higher-TC vs. relatively lower-TC animals, hence the differences observed between the two cholesterol groups were not confounded by the presence of diabetes.

In conclusion, this study demonstrates that systemic hypercholesterolemia and local low ESS are synergistic *in vivo* in promoting the most pronounced progression and high-risk composition of individual coronary lesions. Higher cholesterol levels increase the threshold below which local ESS favors plaque progression in vivo, and they exacerbate plaque growth in arterial regions with similarly low ESS. Combined assessment of cholesterol and local ESS may enhance early identification of coronary regions most likely to exhibit accelerated plaque growth and develop high-risk plaque composition.

Supplementary Material

Refer to Web version on PubMed Central for supplementary material.

Acknowledgments

This work was supported by grants from Novartis Pharmaceuticals Inc and Boston Scientific Inc; the George D. Behrakis Cardiovascular Research Fellowship; the Hellenic Heart Foundation; the Hellenic Atherosclerosis Society, and by NIH RO1 GM49039 (to ERE).

References

1. Nicholls SJ, Tuzcu EM, Crowe T, et al. Relationship between cardiovascular risk factors and atherosclerotic disease burden measured by intravascular ultrasound. J Am Coll Cardiol. 2006; 47:1967–75. [PubMed: 16697312]
2. Libby P, Theroux P. Pathophysiology of coronary artery disease. Circulation. 2005; 111:3481–8. [PubMed: 15983262]
3. Chatzizisis YS, Coskun AU, Jonas M, et al. Role of endothelial shear stress in the natural history of coronary atherosclerosis and vascular remodeling: molecular, cellular and vascular behavior. J Am Coll Cardiol. 2007; 49:2379–93. [PubMed: 17599600]
4. Stone PH, Saito S, Takahashi S, et al. Prediction of progression of coronary artery disease and clinical outcomes using vascular profiling of endothelial shear stress and arterial plaque characteristics: the PREDICTION Study. Circulation. 2012; 126:172–81. [PubMed: 22723305]
5. Wentzel JJ, Chatzizisis YS, Gijsen FJ, et al. Endothelial shear stress in the evolution of coronary atherosclerotic plaque and vascular remodeling: current understanding and remaining questions. Cardiovsc Res. 2012; 96:234–43.
6. Davies PF. Hemodynamic shear stress and the endothelium in cardiovascular pathophysiology. Nat Clin Pract Cardiovasc Med. 2009; 6:16–26. [PubMed: 19029993]
7. Koskinas KC, Chatzizisis YS, Antoniadis AP, Giannoglou GD. Role of endothelial shear stress in stent restenosis and thrombosis. Pathophysiologic mechanisms and implications for clinical translation. J Am Coll Cardiol. 2012; 59:1337–49. [PubMed: 22480478]
8. Papaioannou TG, Karatzis EN, Vavuranakis M, Lekakis JP, Stefanadis C. Assessment of vascular wall shear stress and implications for atherosclerotic disease. Int J Cardiol. 2006; 113:12–8. [PubMed: 16889847]
9. Giannoglou GD, Soulis JV, Farmakis TM, Farmakis DM, Louridas GE. Haemodynamic factors and the important role of local low static pressure in coronary wall thickening. Int J Cardiol. 2002; 86:27–40. [PubMed: 12243848]
10. Samady H, Eshtehardi P, McDaniel MC, et al. Coronary artery wall shear stress is associated with progression and transformation of atherosclerotic plaque and arterial remodeling in patients with coronary artery disease. Circulation. 2011; 124:779–88. [PubMed: 21788584]
11. Cheng C, Tempel D, van Haperen R, et al. Atherosclerotic lesion size and vulnerability are determined by patterns of fluid shear stress. Circulation. 2006; 113:2744–53. [PubMed: 16754802]
12. Simionescu M. Implications of early structural-functional changes in the endothelium for vascular disease. Arterioscler Thromb Vasc Biol. 2007; 27:266–74. [PubMed: 17138941]
13. Hajra L, Evans AI, Chen M, Hyduk SJ, Collins T, Cybulsky M. The NF-kB signal transduction pathway in aortic endothelial cells is primed for activation in regions predisposed to atherosclerotic lesion formation. PNAS. 2000; 97:9052–7. [PubMed: 10922059]
14. Orr AW, Sanders JM, Bevard M, Coleman E, Sarembock IJ, Schwartz MA. The subendothelial extracellular matrix modulates NF-κB activation by flow: a potential role in atherosclerosis. J Cell Biol. 2005; 169:191–202. [PubMed: 15809308]
15. Tzima E, Irani-Tehrani M, Kiosses WB, et al. A mechanosensory complex that mediates the endothelial cell response to fluid shear stress. Nature. 2005; 437:426–31. [PubMed: 16163360]
16. Getz GS, Reardon CA. Animal models of atherosclerosis. Arterioscler Thromb Vasc Biol. 2012; 32:1104–5. [PubMed: 22383700]
17. Koskinas KC, Feldman CL, Chatzizisis YS, et al. Natural history of experimental coronary atherosclerosis and vascular remodeling in relation to endothelial shear stress: a serial, in-vivo intravascular ultrasound study. Circulation. 2010; 121:2092–101. [PubMed: 20439786]
18. Chatzizisis YS, Jonas M, Coskun AU, et al. Prediction of the localization of high risk coronary atherosclerotic plaques on the basis of low endothelial shear stress: an intravascular ultrasound and histopathology natural history study. Circulation. 2008; 117:993–1002. [PubMed: 18250270]
19. Chatzizisis YS, Baker AB, Sukhova GK, et al. Augmented expression and activity of extracellular matrix-degrading enzymes in regions of low endothelial shear stress colocalize with coronary atheromata with thin fibrous caps in pigs. Circulation. 2011; 123:621–30. [PubMed: 21282495]

20. Gerrity RG, Natarajan R, Nadler JL, Kimsey T. Diabetes-induced accelerated atherosclerosis in swine. Diabetes. 2001; 50:1654–65. [PubMed: 11423488]
21. Granada JF, Kaluza GL, Wilensky RL, Biedermann BC, Schwartz RS, Falk E. Porcine models of coronary atherosclerosis and vulnerable plaque for imaging and interventional research. Euro Intervention. 2009; 5:140–8. [PubMed: 19577996]
22. Stone PH, Coskun AU, Kinlay S, et al. Regions of low endothelial shear stress are sites where coronary plaque progress and vascular remodeling occurs in humans: an in-vivo serial study. Eur Heart J. 2007; 28:705–10. [PubMed: 17347172]
23. Coskun AU, Yeghiazarians Y, Kinlay S, et al. Reproducibility of coronary lumen, plaque, and vessel wall reconstruction and of endothelial shear stress measurements in vivo in humans. Catheter Cardiovasc Interv. 2003; 60:67–78. [PubMed: 12929106]
24. Cheruvu PK, Finn AV, Gardner C, et al. Frequency and distribution of thin-cap fibroatheroma and ruptured plaques in human coronary arteries: a pathologic study. J Am Coll Cardiol. 2007; 50:940–9. [PubMed: 17765120]
25. Mintz GS, Nissen SE, Anderson WD, et al. American College of Cardiology clinical expert consensus document on standards for acquisition, measurement and reporting of intravascular ultrasound studies (IVUS). A report of the American College of Cardiology Task Force on clinical expert consensus documents. J Am Coll Cardiol. 2001; 37:1478–92. [PubMed: 11300468]
26. Narula J, Nakano M, Virmani R, et al. Histopathologic characteristics of atherosclerotic coronary disease and implications of the findings for the invasive and noninvasive detection of vulnerable plaques. J Am Coll Cardiol. 2013; 61:1041–51. [PubMed: 23473409]
27. Libby P. Mechanisms of acute coronary syndromes and their implications for therapy. N Engl J Med. 2013; 368:2004–13. [PubMed: 23697515]
28. Tarbel JM. Shear stress and the endothelial transport barrier. Cardiovasc Res. 2010; 87:320–30. [PubMed: 20543206]
29. Vergnani L, Hatrik S, Ricci F, et al. Effect of native and oxidized low-density lipoprotein on endothelial nitric oxide and superoxide production. Key role of l-arginine availability. Circulation. 2000; 101:1261–6. [PubMed: 10725285]
30. Yeh M, Cole AL, Choi J, et al. Role for sterol regulatory element binding protein in activation of endothelial cells by phospholipid oxidation products. Circ Res. 2004; 95:780–8. [PubMed: 15388640]
31. Fang Y, Mohler ER III, Hsieh E, et al. Hypercholesterolemia suppresses inwardly rectifying K^+ channels in aortic endothelium in vitro and in-vivo. Circ Res. 2006; 98:1064–71. [PubMed: 16556870]
32. Libby P, Aikawa M, Kinlay S, Selwyn A, Ganz P. Lipid lowering improves endothelial functions. Int J Cardiol. 2000; 74:S3–10. [PubMed: 10856767]
33. Murase T, Kume N, Korenaga R, et al. Fluid shear stress transcriptionally induces lectin-like oxidized LDL receptor-1 in vascular endothelial cells. Circ Res. 1998; 83:328–33. [PubMed: 9710126]
34. Mohan S, Mohan N, Valente AJ, Sprague EA. Regulation of low shear flow-induced HAEC VCAM-1 expression and monocyte adhesion. Am J Physiol. 1999; 276:C100–7.
35. Ding SF, Ni M, Liu XL, et al. A causal relationship between shear stress and atherosclerotic lesions in apolipoprotein E knockout mice assessed by ultrasound biomicroscopy. Am J Physiol Heart Circ Physiol. 2010; 98:H2121–9. [PubMed: 20382850]
36. Tabas I, Williams KJ, Boren J. Subendothelial lipoprotein retention as the initiating process in atherosclerosis: update and therapeutic implications. Circulation. 2007; 116:1832–44. [PubMed: 17938300]
37. Li D, Mehta JL. Antisense to LOX-1 inhibits oxidized LDL-mediated upregulation of monocyte chemoattractant protein-1 and monocyte adhesion to human coronary artery endothelial cells. Circulation. 2000; 101:2889–95. [PubMed: 10869259]
38. Ogura S, Kakino A, Sato Y, et al. LOX-1, the multifunctional receptor underlying cardiovascular dysfunction. Circ J. 2009; 73:1993–9. [PubMed: 19801851]

39. Stone PH, Feldman CL. In vivo assessment of local intravascular hemodynamics and arterial morphology to investigate vascular outcomes. A growing field coming of age. J Am Coll Cardiol Intv. 2010; 3:1199–201.

40. Nicholls SJ, Puri R. Predicting the future. Challenges moving forward for arterial imaging. Circulation. 2012; 126:161–2. [PubMed: 22723306]

41. Shewan LG, Coats AJS. Ethics in the authorship and publishing of scientific articles. Int J Cardiol. 2010; 144(1):1–2.

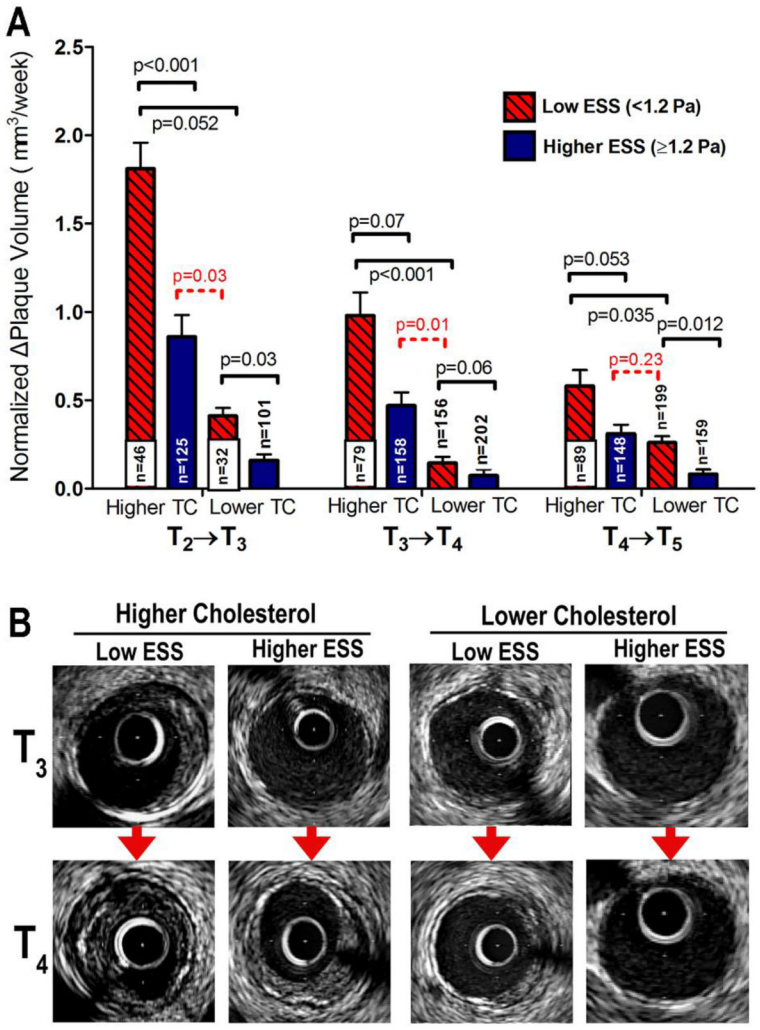

Figure 1.

(**A**) Time-normalized change of plaque volume (nΔPV), for all intervals between consecutive time-points ($T_2 \rightarrow T_3$; $T_3 \rightarrow T_4$; $T_4 \rightarrow T_5$), in segments stratified according to low ESS (<1.2Pa) vs. higher ESS (≥1.2Pa) at each time-point and according to higher-TC vs. relatively lower-TC. Note that segments only from the 36-week cohort (n=304) were analyzed at interval $T_2 \rightarrow T_3$, whereas segments from both the 30-week and 36-week cohort (n=595) were analyzed at intervals $T_3 \rightarrow T_4$ and $T_4 \rightarrow T_5$. (**B**) Representative examples of plaque progression by IVUS between consecutive time-points ($T_3 \rightarrow T_4$) in segments stratified by local ESS and systemic TC categories.

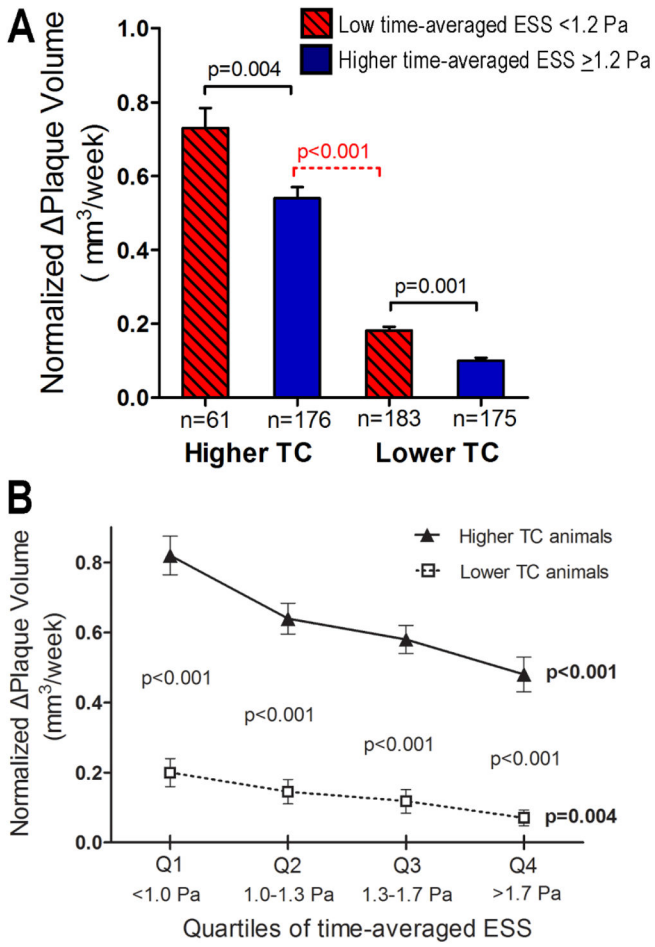

Figure 2.

(A) Time-normalized change of plaque volume (nΔPV) throughout the study period in segments stratified according to low (<1.2Pa) vs. higher time-averaged ESS (≥1.2Pa) and according to higher-TC vs. relatively lower-TC. **(B)** Time-normalized change of plaque volume (nΔPV) throughout the study period across quartiles of time-averaged ESS. P values next to each line, shown in bold, represent the overall association within the corresponding TC category; p values in each ESS quartile represent the difference of nΔPV between higher TC vs. relatively lower TC segments for the given ESS quartile.

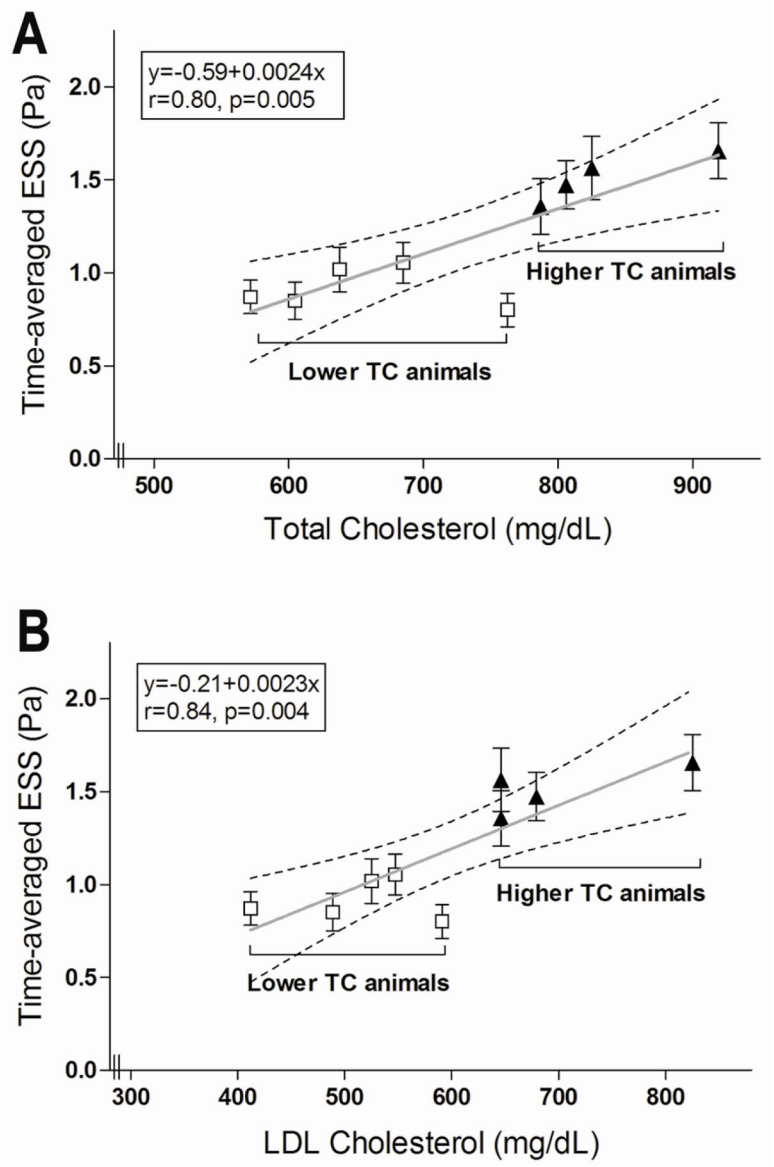

Figure 3.

The time-averaged ESS in segments that culminated in significant plaque by IVUS (defined as maxIMT≥0.5mm by IVUS at follow-up) in each animal is related to the total cholesterol (**A**) and the LDL-cholesterol levels (**B**) in the corresponding animal. Dashed lines represent 95% confidence intervals for the linear regression lines.

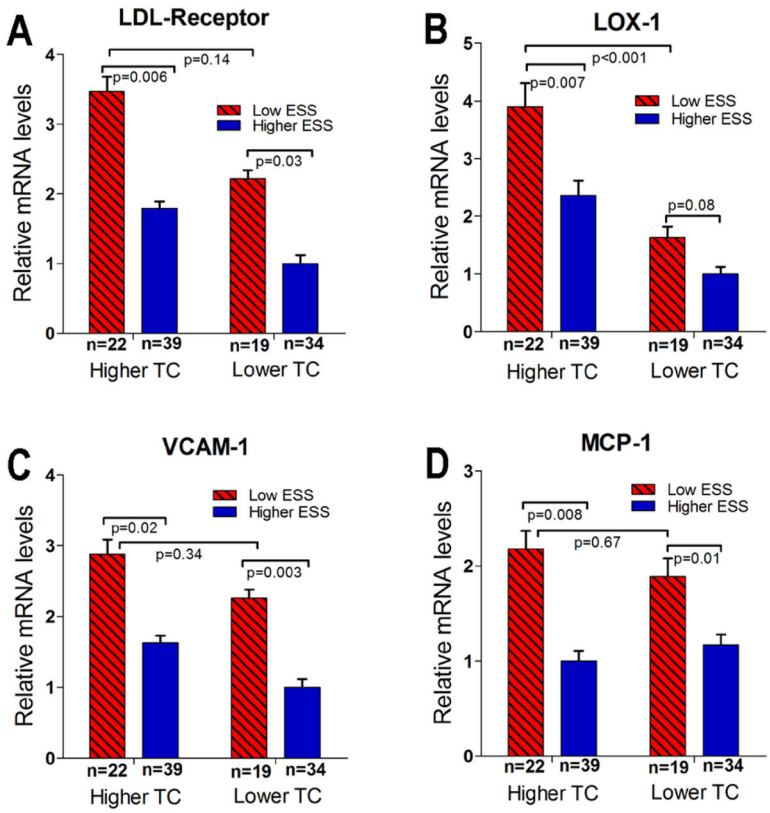

Figure 4.

Relative mRNA levels of the LDL-receptor (**A**), LOX-1 (**B**), VCAM-1 (**C**) and MCP-1 (**D**) in segments with low- vs. higher time-averaged ESS, from higher-TC animals vs. relatively lower-TC animals.

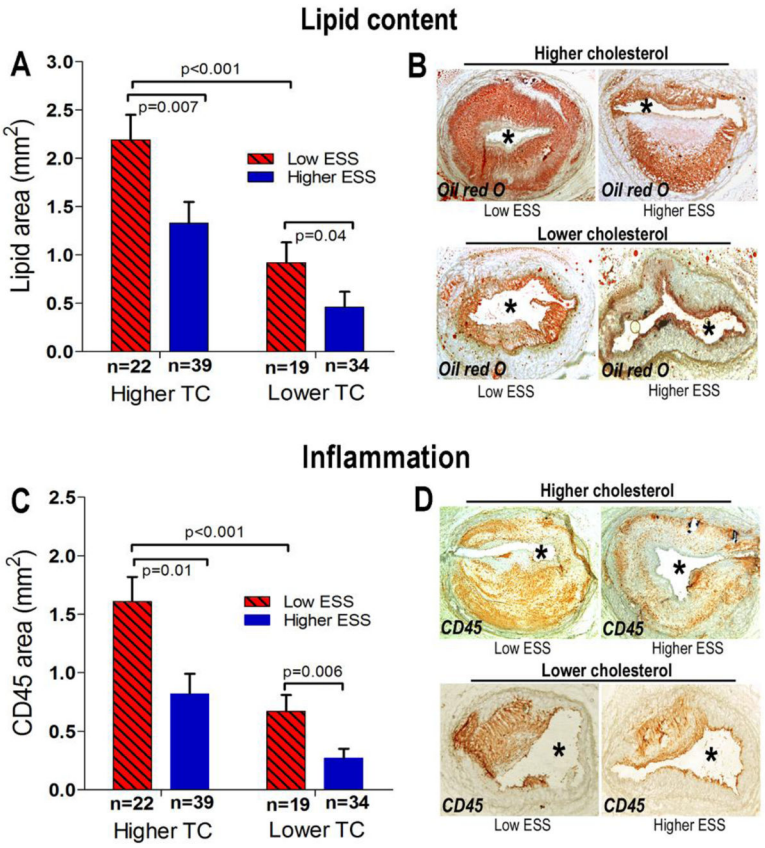

Figure 5.

Quantitative analyses of lipid accumulation (**A**) and CD45-positive leukocyte infiltration (**C**), and representative examples of Oil-red-O staining (**B**) and CD45 immunostaining (**D**) in segments stratified according to time-averaged local ESS (low ESS <1.2Pa vs. higher ESS ≥1.2Pa) and the higher vs. relatively lower cholesterol levels of the corresponding animal.